MINIREVIEW

Container-based multifunctional self-healing polymer coatings

Dmitry G. Shchukin*

The main aim of this minireview is the demonstration of the recent progress achieved in the development of nanocontainer-based self-healing coatings for the protection of metal structures. This minireview covers the reports published within the last three years. Two main types of nanocontainers – polymer capsules and porous composite inorganic nanoparticles loaded with inhibitors or healing agents – are described. The release of the encapsulated active material is achieved by two main triggers: mechanical rupture of the container shell or changes of the local pH in the corroded area. Despite considerable steps made in the field of nanocontainer-based coatings in recent times, challenging problems remain with the mixing of nanocontainers with the coating polymer matrix, effective loading of nanocontainers with inhibitors or healing material and distribution of nanocontainers in the coating matrix.

Introduction to nanocontainer-based self-healing coatings

Self-healing or feedback activity of materials gives information about the gap between the impact and the autonomous response of the materials to this impact. A feedback system can respond to its environment (like local pH-changes during the corrosion process) or an external signal applied to the system (like light or mechanical force). The output is the feedback

Stephenson Institute for Renewable Energy, Department of Chemistry, University of Liverpool, L69 7ZD, Liverpool, UK. E-mail: d.shchukin@liverpool.ac.uk; Tel: +44 (0) 151 7952304

action for a self-healing material restoring its functionality. Feedback active coatings are of great scientific and technological importance, as they can be applied in various fields such as medicine, biotechnology or materials science. Their main, passive function as coatings is to protect the underlying substrate from contact with the environment. In addition to their barrier properties, they also possess active properties due to their active responsive function. A successful approach to impart feedback functionality to a coating is the incorporation of an encapsulated active material in the coating matrix (Fig. 1).[1–3] The versatility of encapsulation technologies, active agents and coating matrixes offer a large number of the coating design strategies.

Mechanical impact is an important external stimulus, which affects coating barrier properties in a negative way by causing microcracks or other damage in the coating. Adopting

Dmitry Shchukin received his diploma in Chemistry (1998) and PhD (2002) from Belarusian State University (Belarus). He was awarded DAAD fellowship (2001), Alexander von Humboldt fellowship (2004), Marie-Curie fellowship (2005), NanoFuture Price (2006) and ForMaT Price (2010) while working at Max Planck Institute of Colloids and Interfaces. He is a professor in chemistry at Stephenson Institute for Renewable Energy, University of Liverpool (UK) and a group leader at Max Planck Institute of Colloids and Interfaces, Potsdam, Germany. His main scientific interests concern hollow nano-containers, feedback active coatings, physico-chemical processes in confined nanoenvironment and interfacial sonochemistry.
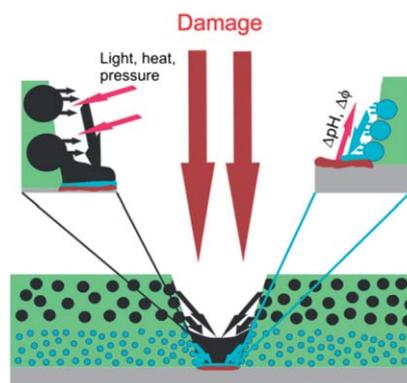

Fig. 1 Schematic representation of nanocontainer-based self-healing coatings. Adapted from ref. 1.

mechanical stress as a trigger to recover the mechanical stability by autonomic crack healing was demonstrated for the first time in 1992 by the group of Dry on the example of using microfibers as carriers for healing agents[4] and then followed in 2001 by the group of S. R. White, where polymer microcapsules were employed for self-healing.[5] They encapsulated a healing agent (dicyclopentadiene) in polymer microcapsules embedded in an epoxy matrix containing a ruthenium-based Grubbs' catalyst. Upon crack formation the embedded microcapsules are ruptured and the healing agent is released in the crack due to capillary forces and comes into contact with the embedded catalyst. The resulting polymerization of the healing agent leads to crack healing and recovery of the barrier properties of the coating. The microcapsules have to be around 50–200 μm to enable easy rupture and sufficient amount of active agent. Other types of first generation self-healing coatings involve poly-electrolyte coatings and the use of large polymer capsules as active coating components.[6,7] Microcapsule shells should be rigid to preserve the capsule integrity during embedding in the coating matrix and brittle to facilitate capsule rupture upon crack formation. However, the integration of big microcapsules into thin coatings is limited because it is not possible to integrate large polymer containers into thin (10–20 μm) coatings. This requests the reduction of the container size and change of the triggering mechanism. Utilizing pH shift as a stimulus for corrosion inhibitor release is a natural promising way to design anticorrosive coatings with sufficient corrosion resistance. That is because the corrosion process leads to local pH decrease in anodic areas and local pH increase in cathodic ones. This triggering mechanism is more suitable for small, nano-containers based on the composite porous inorganic (mostly oxide) scaffold.

Polymer capsules

The first efforts in designing feedback active coatings had been made on the encapsulation of active materials within polymer microcapsules.[5] The main focus in the last three years in this area was devoted to the reduction of microcapsule size simultaneously providing a sensitive polymer shell and the removal of the additional catalyst involved in the healing process by using either humidity or oxygen from the air for polymerization of the healing agent.

Two different self-healing agent candidates, *endo*-dicyclopentadiene (*endo*-DCPD) and 5-ethylidene-2-norbornene (ENB) containing fluorescent dye, were microencapsulated into a melamine–urea–formaldehyde shell by *in situ* polymerization.[8] The spherical microcapsules showed a narrow size distribution and rough outer and smooth inner surfaces for both healing agent systems. Shell thicknesses of the microcapsules were ~880 ± 80 nm for *endo*-DCPD and ~620 ± 60 nm for ENB. Average diameters of *endo*-DCPD- and ENB-microcapsules were found to be ~80 and ~52 μm, respectively. Loading of the healing agent was ~70% for both microcapsules. An epoxy resin-based self-healing system was demonstrated using tungsten(VI) chloride catalyst with a co-activator (phenylacetylene) that initiates ring-opening metathesis polymerization of

dicyclopentadiene.[9] The microcapsules with a diameter of 200 μm and an average wall thickness of 5 μm were synthesized. The concentration of tungsten(VI) chloride catalyst has a significant impact on the virgin properties of the composites and the healing efficiency. The highest healing efficiency 64.9% was obtained with 15 wt% catalyst in self-activated samples. However, the fracture toughness of the capsules decreases with the increase in tungsten(VI) concentration. Considering the high healing efficiency and low diminishment of virgin fracture toughness, the catalyst concentration of 10 wt% was appropriate and the healing efficiency of 59.7% can be obtained. Epoxy resin filled microcapsules were investigated for healing of cracks.[10] Microcapsules were prepared by *in situ* polymerization of urea–formaldehyde resin to form a shell over epoxy resin droplets. Their size was around 100 μm. The model system of self-healing coating consisted of epoxy resin matrix, 10 wt% microencapsulated healing agent and 2 wt% catalyst solution. Diaminodiphenyl sulfone (DDS) was used as a curing agent, adsorbed at the periphery of single-layer microcapsules within melamine–formaldehyde resin.[11] These double-layer microcapsules were made by encapsulating the particulates (the single-layer microcapsules decorated with DDS) with melamine–formaldehyde *via in situ* polymerization. The double-layer microcapsules simultaneously release the healing agent and the curing agent upon the fracture of the surrounding matrix, which increases the rate of contact between the two agents, improving the healing efficiency.

Selvakumar *et al.*[12] reported an *in situ* encapsulation of the healing agent without addition of a catalyst. The urea–formaldehyde capsules were filled with linseed oil as a healing agent and an additional corrosion inhibitor (nanoparticles of CeO_2 and Cr_2O_3). Capsules with diameters as small as 30–40 μm were achieved by *in situ* polymerization in oil-in-water emulsion by stirring. The average content of linseed oil in nanoparticle-loaded microemulsions was 70%. Cracks in paint films were successfully healed when linseed oil and nanoparticles were released from microcapsules ruptured under mechanical action. The crack was gradually reduced and completely filled after 90 s. Linseed oil undergoes drying by oxidation with atmospheric oxygen, forming a continuous film within the crack. In the proximity of the local damage, both the anodic metal dissolution and the cathodic oxygen reduction showed that the coating with microcapsules at 4% concentration substantially and spontaneously decreased the rate of corrosion.[13] Electrochemical impedance measurements underlined the protective effect of the coating as well.

Another application of linseed oil as a healing agent was described in ref. 14. Phenol–formaldehyde microcapsules with linseed oil as an active agent were produced by *in situ* polymerization. At low agitation rates (200–400 rpm), the obtained microcapsules were relatively large in the range of 100–150 μm. At higher rates (600 rpm), microcapsules with an average diameter of 50–60 μm were obtained, and their shell wall was found to be more uniform, which might be because of increased interfacial area and more homogeneous reaction. The microcapsules were uniformly mixed, without any damage to the epoxy matrix, by stirring at 200 rpm for 20 min. The coatings

with microcapsules were found to be free from corrosion and blistering at the scribed lines after 72 h of immersion in NaCl solution. In contrast, specimens without microcapsules rapidly corroded within 48 h and exhibited extensive rust formation. It was found that an increase in stirring rate, correct choice of temperature, and a high stabilizer concentration all caused a decrease in microcapsule size but was accompanied by excessive formation of nanoparticles.[15] However, high agitation rate is not possible because too vigorous agitation caused capsules to reside high up on the sides of the reactor thereby not participating in reaction anymore, not building up the required wall thickness and leaving the excess of shell material in the reaction mass. Ultrasonic application also reduces the size of capsules.[16] The applied ultrasonic energy broke the linseed oil droplets into finer ones with smaller spherical surfaces for the polymerization of urea and formaldehyde also providing better adhesion of the smaller capsules to the coating matrix.

There are also several demonstrations of using other healing agents, which do not require an additional catalyst for curing, for encapsulation inside polymer containers. Polyurethane microcapsules containing hexamethylene diisocyanate were manufactured *via* interfacial polymerization reaction of commercial methylene diphenyl diisocyanate prepolymer and 1,4-butanediol in an oil-in-water emulsion.[17] Isocyanates are reactive with moisture and can be used as catalyst-free healing agents. The capsules had diameters of 5–350 μm and shell thicknesses of 1–15 μm. The shell wall thickness is roughly uniform and in the micrometer level, which acts as an appropriate barrier from leakage and provides enough mechanical stiffness from rupture during curing inside the coating matrix. The typical core fraction of microcapsules and the yield of synthesis were around 60 wt%.

From the SEM images of the scratched area of the coated panels (Fig. 2), it is seen that newly formed materials filled the crack. The crack was sealed and healed autonomously to retard the diffusion of salt ions and thus protect the substrate from the corrosion process. The materials generated in the crack are the product between hexamethylene diisocyanate released from ruptured microcapsules and water. As a comparison, it could be seen that the crack of the control specimen was not sealed and severe rust was observed.

Another example for catalyst-free self-healing materials is the use of a reactive silyl ester as an organic reactive healing agent encapsulated inside polymer containers.[18] Silyl esters present the capability to react with water/humidity and metallic substrates, forming a metal barrier hydrophobic system which protects the metal at the scribe from further corrosion attacks. A hydrolysable organic silane, perfluorooctyl triethoxysilane, was also selected and microencapsulated as a healing agent.[19] Organic silane molecules tend to hydrolyze in a wet environment and crosslink to form a solid film. Encapsulated $1H,1H,2H,2H$-perfluorooctyl triethoxysilane is commercially available, hydrophobic and forms hydrophobic films from hydrolysis and polycondensation, which will repel aqueous electrolyte solution away from metal thus providing further corrosion protection. The average diameter of microcapsules was 50 μm with a core fraction around 60%. The scratched area of the steel panel coated with silane-based self-healing coating was free of rust after 48 h immersion in the NaCl solution whereas the control sample without silane-loaded microcapsules was completely degraded. Another mixture of alkoxysilanes (trimethoxy(octadecyl)silane and trimethoxy(octyl) silane) was demonstrated as a healing agent.[20] All control samples without silane-loaded microcapsules showed the corrosion onset already 6 hours after immersion in 0.1 M NaCl solution. In contrast, the self-healing samples with 6 wt% microcontainers loaded with alkoxysilanes showed no visual evidence of corrosion even 3 days after exposure to NaCl solution. Alkoxysilanes can be easily replaced to corrosion inhibitor methylbenzothiazole.[21]

A very interesting approach for the preparation of multifunctional emulsion-based microcontainers was demonstrated using Pickering emulsion particles as a carrier of two corrosion inhibitors.[22] The silica armoured polystyrene (PS) composite nanocontainers filled with 5, 10, or 20 wt% of corrosion inhibitor 8-hydroxyquinoline (8HQ) were demonstrated and further extended to the encapsulation of other organic corrosion inhibitors like mercaptobenzothiazole (MBT) or benzotriazole. The aim of the work was to introduce a new type of functional particle based on Pickering emulsions as multifunctional containers with a one-pot fabrication protocol. SEM visualizations of silica–PS–8HQ and silica–PS–MBT composites prepared by ultrasonication are shown in Fig. 3. The spherical composite nanocontainer shell consisted of densely packed silica nanoparticles. By varying the silica nanoparticle mass fraction, the nanocontainer size can be easily controlled and decreased to a minimum of around 200 nm. The transfer of the synthesized silica–PS–inhibitor composite capsules into the alkyd coating can be performed directly from the suspension or from the dried powder of the nanocontainers by the dispersion with a rotor-stator mixing device (Ultra-Turrax). The films with silica–PS nanocontainers exhibited higher impedance after 6 days as compared with the blank films. However, the films with
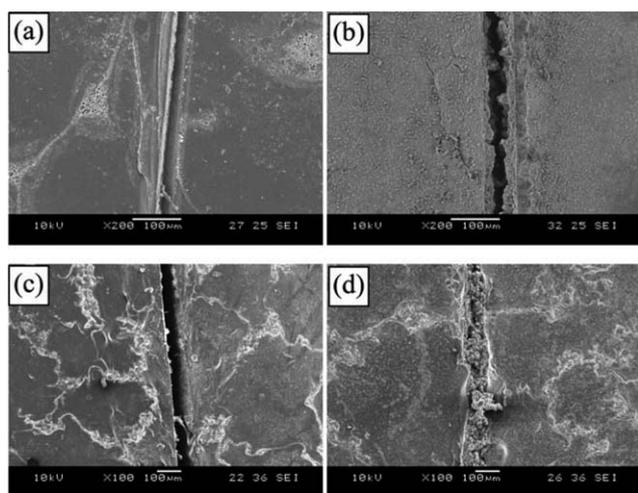

Fig. 2 SEM images of the scratched regions before immersion (a: control coating, c: self-healing coating) and after immersion in salt water for 48 h (b: control coating, d: self-healing coating). Reproduced from ref. 17.
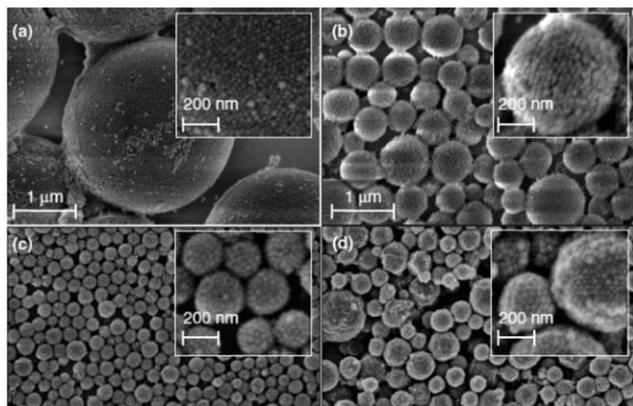
Fig. 3 SEM micrographs of silica–PS–8HQ composite nanocontainers for different silica-mass to oil-volume ratios (a) 0.09, (b) 0.32, and (c) 0.91 g mL^{-1}. (d) Silica–PS–MBT composite nanocontainers. Adapted from ref. 22.

8-hydroxyquinoline doped silica–polystyrene nanocontainers had higher impedances than the films containing silica–polystyrene nanocontainers without 8-hydroxyquinoline due to the additional passivation on the aluminium surface caused by the release of 8-hydroxyquinoline inside the microcracks of the coating.

Composite inorganic nanocontainers

The second type of containers employed in the self-healing coatings is based on the use of the composite polymer–inorganic nanocontainers with inorganic scaffolds. Most of the scaffolds are mesoporous nanoparticles (SiO$_2$, TiO$_2$, CeO$_2$ and some other oxides), natural halloysite nanotubes and ion-exchange clays like layered double hydroxides. The outer surface of the inorganic containers can be coated with a pH-sensitive polyelectrolyte (*e.g.*, weak polyelectrolytes) or polymer (*e.g.*, polyacrylates) shell to provide controlled release of the encapsulated inhibitor. The main advantage of the composite inorganic nanocontainers is their small size (in most cases below 1 μm), which allows one to use them in thin coatings. The triggering mechanism of the inhibitor release is in most cases the local changes of the pH value caused by the corrosion process, which impacts the sensitive polymer or the polyelectrolyte shell to open the pores and release inhibitor encapsulated in the porous interior. However, the use of other triggers like external light[23,24] or changes of the local electrochemical potential[25] was also demonstrated. The major drawback of such containers is that the loading capacity is quite low due to their inner mesoporous structure. While polymer microcapsules usually have 50–60 wt% of the loading of healing agent, ceramic containers can provide 20–30 wt% and, in very rare cases, 50–60 wt% can be achieved.

Ion-exchange clay nanoparticles were probably the first composite inorganic nanocontainers introduced into self-healing coatings. The indole-3-butyric acid (IBA)-modified montmorillonite clay improved the corrosion performance of epoxy coatings on the carbon steel.[26] The carbon steel covered by the pure epoxy coating was strongly corroded after 7 days of immersion in NaCl solution. In contrast the sample containing IBA-modified clay had the same appearance as before immersion: there was no corrosion product. The inhibitor release from the IBA-modified clay was favoured for high pH values. When the pH increased and became higher than the pK_a = 4.9 of IBA, the nitrogen function was no more charged and the interactions between the clay and the inhibitor were reduced. This can explain the increase of the inhibitor release for pH higher than 5. Rare earth metal salts were shown to be effective corrosion inhibitors on a wide range of metals including hot dip galvanized steel. The composite montmorillonite clay was modified by Ce(III) ions to obtain Ce(III) montmorillonite clay nanocontainers.[27] The release of Ce ions was triggered by the presence of sodium or zinc ions. In 0.1 M NaCl solution, the amount of leached cerium was very low (∼6 to 7% of the amount incorporated in the clay). For the same ionic strength, replacing Na$^+$ by Zn^{2+} cations leads to an increase of the amount of leached cerium to >25%. The corrosion inhibitor–inorganic clay composite including benzoate anion intercalated Zn–Al layered double hydroxides (LDHs) was assembled by co-precipitation.[28] The benzoate anion was successfully intercalated into the LDH interlayer and the benzene planes were vertically bilayer-positioned as a quasi-guest ion-pair form in the gallery space. A slow and persistent release was observed based on the ion-exchange process between the benzoate anion pillared in the LDH lamella host and the chloride anion in 3.5% NaCl solution indicating a significant reduction of corrosion rate observed when the LDH nanohybrid is present in the corrosive medium. The synthesis of the composite layered double hydroxide nanocontainers loaded with different corrosion inhibitors (vanadate – VO$_x$, phosphate – H$_x$PO$_4$ and mercaptobenzothiazolate – MBT) was presented.[29,30] The particle diameter was on the order of 200–400 nm and lateral size 20–40 nm. The best protection results were found for combinations of different LDHs inside polymer coating. For the LDH–H$_x$PO$_4$/LDH–VO$_x$ system, the aluminium alloy surface was slightly changed, upon which only very small defects covered with dense deposits can be detected. Similar results were also found for the aluminium specimen immersed in electrolyte with LDH–MBT/LDH–VO$_x$. In the latter case corrosion products and passivated pits were absent and only some yellowish areas were detected, probably because of the formation of protective films with MBT and VO$_x$. Measurements of the electrochemical impedance of the coatings are in agreement with visual analysis of the metallic substrates indicating a positive effect of combinations of different nanocontainer/inhibitor systems. Another research work of this group presented a very simple approach that can be used to grow spatially differentiated composite Zn–Al LDHs *in situ* on the surface of aluminium alloys.[31] The methodology explores the weakness of the native aluminium oxide layer in the zones of intermetallic phases which are the most susceptible for localized corrosion attacks. The source of aluminium cations necessary to grow the LDHs on the alloy surface is uneven, promoting differentiated growth of island-like LDHs on active intermetallics. The loading of corrosive inhibitor into the intergallery space of LDH by ion exchange reaction created nanostructured container islands on the active zones.

Mesoporous nanoparticles were extensively studied in the last three years for the Royal application in self-healing coatings and considerable progress was achieved. Monodisperse, mesoporous silica nanoparticles were loaded with corrosion inhibitor benzotriazole and embedded in hybrid sol–gel coating for the corrosion protection of aluminium alloy.[32] The developed mesoporous silica–benzotriazole system exhibited high surface area ($\sim$1000 m^2 g^{-1}), narrow pore size distribution ($d \sim$ 3 nm), large pore volume ($\sim$1 mL g^{-1}) and high loading capacity for benzotriazole (41 wt%). Mesoporous silica nanoparticles store the corrosion inhibitor and prevent it from undesired leakage and contact with the coating matrix. Similar application of the mesoporous silica nanoparticles was demonstrated for sol–gel coatings showing the effective corrosion protection in alkaline media and for solvent-based polyester coatings.[33,34] Functional nanocontainers based on silica nanocapsules of 100 nm diameter synthesized and loaded with corrosion inhibitor mercaptobenzothiazole in a one-stage process were reported.[35] Mesoporous nanocapsules possess an empty core and shell with gradual mesoporosity, which confers significant loading capacity and allows prolonged and stimuli-triggered release of the inhibiting species.

The effect of the concentration of embedded nanocontainers on the coating anticorrosion efficiency was determined to be a critical factor.[36] It was found that incorporating inhibitor-loaded silica nanocontainers is not always favourable for the anticorrosion performance of the coating. Embedding nanocontainers at very low concentrations (0.04 wt%) led to good coating barrier properties but no satisfactory corrosion inhibition because of an insufficient amount of available inhibitor. In comparison, too high inhibitor-loaded nanocontainer concentrations deteriorate the coating integrity by introducing diffusion paths for aggressive electrolyte species, which results in a loss of anticorrosion efficiency. Therefore, to obtain protective coatings with optimum anticorrosive properties, a compromise between coating integrity and active corrosion inhibition should be found.

Composite cerium molybdate nanocontainers were synthesized using a two-step process and then loaded with 8-hydroxyquinoline (loading 5 wt%) or with 1-*H*-benzotriazole-4-sulfonic acid (loading 16 wt%).[37] First, polystyrene nanospheres were produced using emulsion polymerization. Second, the polystyrene spheres were coated *via* the sol–gel method to form a cerium molybdate layer. Finally, the nanocontainers were obtained by calcination of cerium molybdate coated polystyrene nanospheres. After calcination of the coated nanospheres, the resulting nanocontainers were modified with loading the inhibitor. Application of cerium molybdate nanocontainers loaded with mercaptobenzothiazole was shown for the protection of magnesium alloys.[38] The containers were additionally loaded with mercaptobenzothiazole (58 wt%) thus consisting of two corrosion inhibitors – cerium molybdate and mercaptobenzothiazole.

SEM surface mapping was taken for the organosilicate coating including loaded containers in order the well dispersion of the containers into the film to be estimated. The elemental cerium mapping micrograph and the corresponding SEM image

of organosilicate coating loaded with cerium molybdate – mercaptobenzothiazole nanocontainers – are demonstrated in Fig. 4. Spots of cerium element can be clearly seen in the pictures. The containers are quite well dispersed in the coating. The organic coating performed improved corrosion protection properties after exposure to 0.5 M NaCl solution for 4 months. Studies on artificial defected coatings immersed in 1 mM NaCl solution for 73 h presented partial self-recovery of the films. Two different polymer coatings were prepared, one including 4 wt% nanocontainers loaded with mercaptobenzothiazole and another one including 10 wt% nanocontainers loaded with mercaptobenzothiazole.[39] It was clearly found from the electrochemical impedance values that 4% of the loaded nanocontainer coating demonstrated considerably better corrosion protective behaviour after 744 h of exposure in the corrosive environment than that for the coating with 10% of loaded nanocontainers. The reason is that the 10 wt% of containers formed agglomerates in the coating that produce conductive pathways for electrolyte reaching the substrate. A spontaneous emulsification method was exploited to prepare mesoporous CeO$_2$@SiO$_2$ hybrid particles and their incorporation into a silica–zirconia coating to improve the corrosion protection of aluminium.[40] As a synthesis method, spontaneous emulsification has the advantage of requiring neither externally applied energy nor stabilizing or templating species. To complement CeO$_2$ corrosion inhibition, 8-hydroxyquinoline was used, which is an effective anodic inhibitor that exhibited synergistic effects with Ce-containing compounds. These two encapsulated inhibiting species provided effective corrosion protection of aluminium by two mechanisms: the initial burst of encapsulated 8-hydroxyquinoline followed by the sustained release of the Ce ions.

A new material for synthesis of mesoporous nanocontainers introduced within the last three years is the composites based on titanium dioxide. Epoxy coatings containing TiO$_2$ nanocontainers were applied on aluminium alloy 2024-T3 for corrosion protection.[41] The nanocontainers were hollow with sizes ranging from 150 nm to 270 nm. The incorporation of TiO$_2$-based nanocontainers loaded with 8-hydroxyquinoline into epoxy coatings totally changed the behaviour of the films. The total impedance value was significantly increased in the case of the polymer coatings with nanocontainers.

Halloysite clay tubes of 50 nm diameter and *ca.* 1000 nm length were analysed as potential nanocontainers for loading
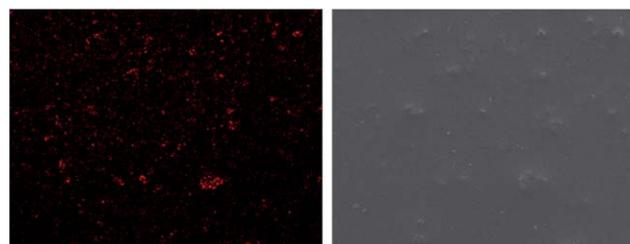

Fig. 4 Mapping micrograph (left) and corresponding SEM image (right) of nanocontainer-impregnated coating. Reproduced from ref. 38.

inside their interior, storage and induced sustained release of active materials.[42,43] Halloysite nanotubes loaded with the corrosion inhibitor benzotriazole can be admixed into polymer epoxy coating to improve its anticorrosion performance as well as coating tensile strength. For formation of the tube end stoppers, benzotriazole loaded halloysite was exposed to the solution of Cu(II) ions. A typical loading efficiency of benzotriazole was in the range 6–9% by volume which is close to the total lumen volume of *ca.* 10% of the tube. A slow corrosion of the metal substrate for coatings with loaded halloysites was taking place only at the initial stage, but this process was almost completely suppressed due to the benzotriazole release from the halloysites.

Conclusions

There are a number of promising approaches developed in the last 3 years for self-healing coatings, but one has to be aware that there are also other parameters that finally decide if these can be marketed. There are both technical issues if, for example, mechanical properties, adhesion, and optical appearance are not affected by coating, and socio-economic criteria like low cost, environmentally friendliness that have to be considered. Therefore, even this rather conventional case requires a multidisciplinary and multitechnological approach to arrive at a specific application. On the other hand, the progress in the last few years has been fast and encouraging that one can be confident to find solutions applicable for different types of coatings.

Much research is needed on the level of understanding the interplay of structural hierarchies. This requires more sophisticated preparative and analytical methods covering different length scales. There are examples in materials and in biology and these disciplines can cross-fertilize each other. From another point of view, much of what was learnt with self-healing functionality can be transferred to others like friction and antifungal. Therefore, one can expect a drastic expansion of the field of nanocontainer-based self-healing materials. Many of the ideas will remain phantasy once it comes to practical applications, but even a small fraction of surviving approaches will make this a prospering field.

Notes and references

1 D. G. Shchukin and H. Möhwald, *Small*, 2007, **3**, 926–943.
2 D. G. Shchukin, D. O. Grigoriev and H. Möhwald, *Soft Matter*, 2010, **6**, 720–725.
3 D. G. Shchukin and H. Möhwald, *Chem. Commun.*, 2011, **47**, 8730–8739.
4 C. M. Dry, *Proc. SPIE*, 1992, **1777**, 367–371.
5 S. R. White, N. R. Sottos, P. H. Geubelle, J. S. Moore, M. R. Kessler, S. R. Sriram, E. N. Brown and S. Viswanathan, *Nature*, 2001, **409**, 794–797.
6 P. Bertrand, A. Jonas, A. Laschewsky and R. Legras, *Macromol. Rapid Commun.*, 2000, **21**, 319–348.
7 A. Kumar, L. D. Stephenson and J. N. Murray, *Prog. Org. Coat.*, 2006, **55**, 244–253.
8 H. H. Noh and J. K. Lee, *eXPRESS Polym. Lett.*, 2013, **7**, 88–94.
9 L. Haiyan, W. Rongguo and L. Wenbo, *J. Reinf. Plast. Compos.*, 2012, **31**, 924–932.
10 Z. Yang, Z. Wei, L. Le-ping, W. Si-jie and L. Wu-jun, *Appl. Surf. Sci.*, 2012, **258**, 1915–1918.
11 R. Tian, X. Fu, Y. Zheng, X. Liang, Q. Wang, Y. Ling and B. Hou, *J. Mater. Chem.*, 2012, **22**, 25437–25446.
12 N. Selvakumar, K. Jeyasubramanian and R. Sharmila, *Prog. Org. Coat.*, 2012, **74**, 461–469.
13 A. Pilbáth, T. Szabó, J. Telegdi and L. Nyikos, *Prog. Org. Coat.*, 2012, **75**, 480–485.
14 R. S. Jadhav, D. G. Hundiwale and P. P. Mahulikar, *J. Appl. Polym. Sci.*, 2011, **119**, 2911–2916.
15 T. Nesterova, K. Dam-Johansen, L. T. Pedersen and S. Kiil, *Prog. Org. Coat.*, 2012, **75**, 309–318.
16 S. H. Bouraa, M. Peikari, A. Ashrafi and M. Samadzadeh, *Prog. Org. Coat.*, 2012, **75**, 292–300.
17 M. Huang and J. Yang, *J. Mater. Chem.*, 2011, **21**, 11123–11130.
18 S. J. García, H. R. Fischer, P. A. White, J. Mardel, Y. González-García, J. M. C. Mol and A. E. Hughes, *Prog. Org. Coat.*, 2011, **70**, 142–149.
19 M. Huang, H. Zhang and J. Yang, *Corros. Sci.*, 2012, **65**, 561–566.
20 A. Latnikova, D. O. Grigoriev, J. Hartmann, H. Möhwald and D. G. Shchukin, *Soft Matter*, 2011, **7**, 369–372.
21 A. Latnikova, D. O. Grigoriev, M. Schenderlein, H. Möhwald and D. G. Shchukin, *Soft Matter*, 2012, **8**, 10837–10844.
22 M. F. Haase, D. O. Grigoriev, H. Möhwald and D. G. Shchukin, *Adv. Mater.*, 2012, **24**, 2429–2435.
23 E. V. Skorb, D. V. Sviridov, H. Mohwald and D. G. Shchukin, *Chem. Commun.*, 2009, 6041–6043.
24 E. V. Skorb, A. G. Skirtach, D. V. Sviridov, D. G. Shchukin and H. Mohwald, *ACS Nano*, 2009, **3**, 1753–1760.
25 D. G. Shchukin, K. Kohler and H. Mohwald, *J. Am. Chem. Soc.*, 2006, **128**, 4560–4561.
26 T. T. X. Hang, T. A. Truc, M.-G. Olivier, C. Vandermiers, N. Guérit and N. Pébère, *Prog. Org. Coat.*, 2010, **69**, 410–416.
27 C. Motte, M. Poelman, A. Roobroeck, M. Fedel, F. Deflorian and M.-G. Olivier, *Prog. Org. Coat.*, 2012, **74**, 326–333.
28 Y. Wang and D. Zhang, *Mater. Res. Bull.*, 2011, **46**, 1963–1968.
29 J. Tedim, S. K. Poznyak, A. Kuznetsova, D. Raps, T. Hack, M. L. Zheludkevich and M. G. S. Ferreira, *ACS Appl. Mater. Interfaces*, 2010, **2**, 1528–1535.
30 M. F. Montemor, D. V. Snihirova, M. G. Taryba, S. V. Lamaka, I. A. Kartsonakis, A. C. Balaskas, G. C. Kordas, J. Tedim, A. Kuznetsova, M. L. Zheludkevich and M. G. S. Ferreira, *Electrochim. Acta*, 2012, **60**, 31–40.
31 J. Tedim, M. L. Zheludkevich, A. N. Salak, A. Lisenkov and M. G. S. Ferreira, *J. Mater. Chem.*, 2011, **21**, 15464–15470.
32 D. Borisova, H. Möhwald and D. G. Shchukin, *ACS Nano*, 2011, **5**, 1939–1946.
33 T. Chen and J. J. Fu, *Nanotechnology*, 2012, **23**, 505705.
34 M. J. Hollamby, D. Fix, I. Dönch, D. Borisova, H. Möhwald and D. G. Shchukin, *Adv. Mater.*, 2011, **23**, 1361–1365.

35 F. Maia, J. Tedim, A. D. Lisenkov, A. N. Salak, M. L. Zheludkevich and M. G. S. Ferreira, *Nanoscale*, 2012, **4**, 1287–1298.

36 D. Borisova, H. Möhwald and D. G. Shchukin, *ACS Appl. Mater. Interfaces*, 2012, **4**, 2931–2939.

37 I. A. Kartsonakis and G. Kordas, *J. Am. Ceram. Soc.*, 2010, **93**, 65–73.

38 I. A. Kartsonakis, A. C. Balaskas, E. P. Koumoulos, C. A. Charitidis and G. Kordas, *Corros. Sci.*, 2012, **65**, 481–493.

39 I. A. Kartsonakis, A. C. Balaskas, E. P. Koumoulos, C. A. Charitidis and G. Kordas, *Corros. Sci.*, 2012, **57**, 30–41.

40 M. J. Hollamby, D. Borisova, H. Möhwald and D. G. Shchukin, *Chem. Commun.*, 2012, **48**, 115–117.

41 A. C. Balaskas, I. A. Kartsonakis, L.-A. Tziveleka and G. Kordas, *Prog. Org. Coat.*, 2012, **74**, 418–426.

42 E. Abdullayev and Y. Lvov, *J. Mater. Chem.*, 2010, **20**, 6681–6687.

43 A. Joshi, E. Abdullayev, A. Vasiliev, O. Volkova and Y. Lvov, *Langmuir*, 2013, DOI: 10.1021/la3044973, in print.